Digital filtering schemes for data processing of test beam of the prototype of the LumiCal detector.

Evgenii Lutsenko[1,*]

[1]Joint Institute of Nuclear Research, Russia

Abstract. The LumiCal electromagnetic calorimeter is designed for the forward region of future electron-positron colliders, such as CLIC and ILC. It is intended to improve hermetically of detectors by detecting electrons, positrons, and photons at small angles. Currently, the detector prototypes are studied in the beam test conditions. An important part of the signal processing is the digital filtering implemented in the read-out electronics, influencing the precision and quality of gathered data. In this article three schemes of digital filtering of gathered signal from test beam for the LumiCal detector prototype are presented.

1 Introduction

Future electron-positron colliders in the TeV range (ILC[1], CLIC[2]) are designed to provide access to possible physics effects beyond Standard Model or to confirm its reliability. The main tasks of e^+e^- colliders are: studies of the Higgs boson (in processes $e^+e^- \rightarrow f\bar{f}H$), high-precision measurements of the top quark properties, Supersymmetry studies. Electrons on small angles are necessary detected for research those processes. One of detectors is the electromagnetic calorimeter LumiCal[3], which prototype is currently being designed and tested.

2 TestBeam 2016 for LumiCal detector prototype

LumiCal is an elecromagnetic Si-W sandwich segmented calorimeter at small angles ($\theta_{inner} = 30.4 mrad$; $\theta_{outer} = 111.5 mrad$). The plate design is shown in the lest part of figure 1a. It is served by two read-out APV chips. One chip includes a preamplifier and shaper, an analog pipeline and a deconvolution filter for each of its 128 channels.

A schematic layout of the experimental setup for testing the prototype of the LumiCal electromagnetic calorimeter is shown in figure 1b. In the test beam setup a prototype of this detector was used, consisting of several plates which are located one after another. The first two segments are 'tracker' - a part of detector prototype, which has no tungsten. The last six plates are detector. In total, 2048 channels for data reading were used in this experimental setup. A bunch of electrons passes through the mesh then they radiate photons. In a magnetic field, these beams are separated and fall into the LumiCal detector prototype.

*e-mail: lutsenko.evg.ol@gmail.com

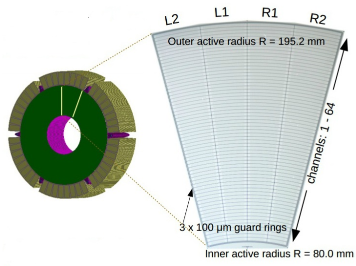

(a)

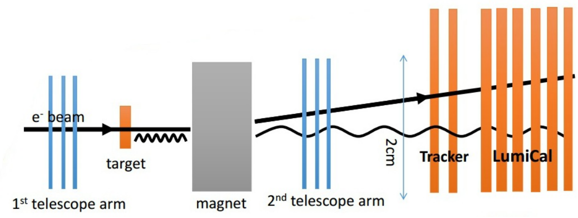

(b)

Figure 1: One section of the prototype detector LumiCal (a). A Schematic layout of the test beam 2016 for LumiCal (b).

3 Digital filter schemes

The readout scheme for time and amplitude measurements is present on figure 2. The scheme show that sensor current is converted in analog signal after shaper, which produces a signal in the form of the Landau distribution. and after that it is digitized. The signal approximately the same amplitude as the charge value and signal-to-noise ratio is improved. Digital filtering is required to restore the original signal. Schematically this is shown on the right side of figure 2.

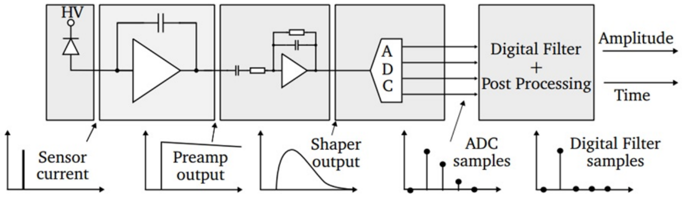

Figure 2: Block diagram of the proposed readout scheme.

3.1 Fitting scheme

The standard scheme (baseline approach) for a digital filter is fitting time scan in a channel and definition a maximum of the function (figure 3a).

$$F(t) = \frac{A(t - t_0)}{\tau} e^{1-(t-t_0)/\tau}, \tag{1}$$

where τ is shaping time, t_0 is pulse occurrence time, A is the fit function amplitude and equal A_{fit}.

3.2 Signal integration scheme

An alternative to baseline approach of digital filtering was developed. It consists in parametrizing a maximum value of shaped signal (A_Σ) with Σ in each channel(figure 3b).

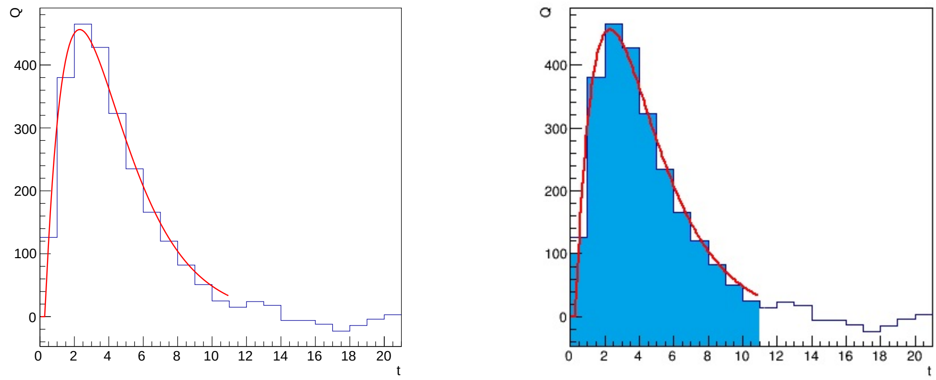

(a) (b)

Figure 3: A signal of one channel with the result of fitting (a). The signal with the result of fitting (red line) and the area that is equal to the Σ (filled area) (b).

To compare the two quantities, the dependence of the maximum value (Q_{max}) on the sum of the values(Σ) in the bins on the time (t) development is plotted. Each point on figure 4 corresponds to the signal from figure 3a. After that, this dependence fits with the function $S(\Sigma)$.

$$A_{\Sigma} = S(\Sigma) = A + \sqrt{B + C\Sigma}. \tag{2}$$

This kind of function was chosen because Σ and $\int F(t)dt$ have the same meaning. The dependence between the original function and its integral is the square root. The red line on figure 4 is the alternative scheme for digital filtering Because each Σ corresponds to a specific value A_{Σ}.

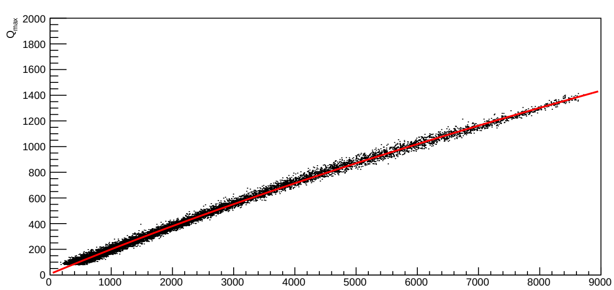

Figure 4: Correlation between the maximum value and the sum.

Similar to the Signal integration scheme, for the fit scheme can calculate the integral of a function in a certain interval and compare it with the amplitude of the fit function (A_{fit}). The histogram will be almost identical to figure 4.

3.3 Deconvolution scheme

The digital filter is one of the important steps of reading the signal from the detector. For these tests, the finite impulse response filter was used. In figure 5a[4] the green line is an analog signal. But for future data processing, there are only specific data read after regular time intervals, which are marked by black dots. For used APV-chips, there is some mathematical transformation that allows the original signal amplitude from the data is restored. First of all, it is necessary to determine two nonzero values(s_1, s_2) from which the pulse occurrence time(t_0) and amplitude of the analog signal(A_{dec}) are calculated (red dots in figure 5). This method is described in more detail in the dissertation [4].

$$t_0 = \frac{s_2/s_1 T_{smp}}{s_2/s_1 + e^{-\frac{T_{smp}}{\tau}}}. \tag{3}$$

$$A_{dec} = (s_1 + s_2)\frac{\tau e^{\frac{T_{smp}-t_0-\tau}{\tau}}}{(T_{smp} - t_0(1 - e^{\frac{T_{smp}}{\tau}}))}. \tag{4}$$

Initially, the function that performs deconvolution was tested on the artificial signal generator

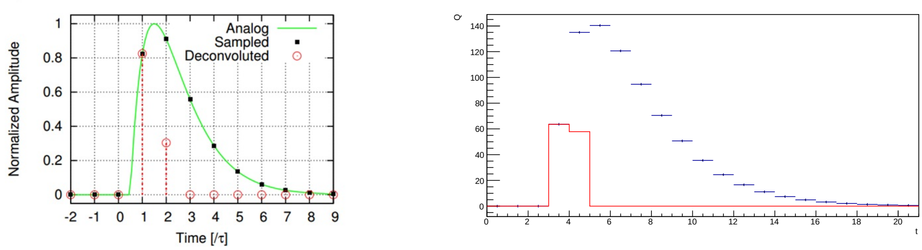

(a) (b)

Figure 5: Deconvolution filter response (a). Example of method test on the signal generator (b).

which was specifically developed for the test beam 2016 of the LumiCal detector prototype. The test amplitudes of pulses were correctly determined using the deconvolution method. An example of one of the tests is presented in figure 5. Processing of real raw data from beam tests was difficult. Because the whole theory is built on ideal conditions, and when tests have noise, then all deconvolution points have a nonzero value. As a solution to this, the amplitude was calculated for each consecutive pair of points. As the correct amplitude, the maximum was taken. It turned out that for each data there is a preferential pair of values from which the finite amplitude can be correctly calculated.

3.4 Correlations

The next step after the development and testing of two alternative methods for correctness was the construction of the correlation histograms of these methods relative to the baseline. Figure 6 shows examples of the histogram of $A_{fit} - A_{alternative}$ dependence on A_{fit} for a channel with a signal, where $A_{alternative}$ is A_{Σ} or A_{dec}.

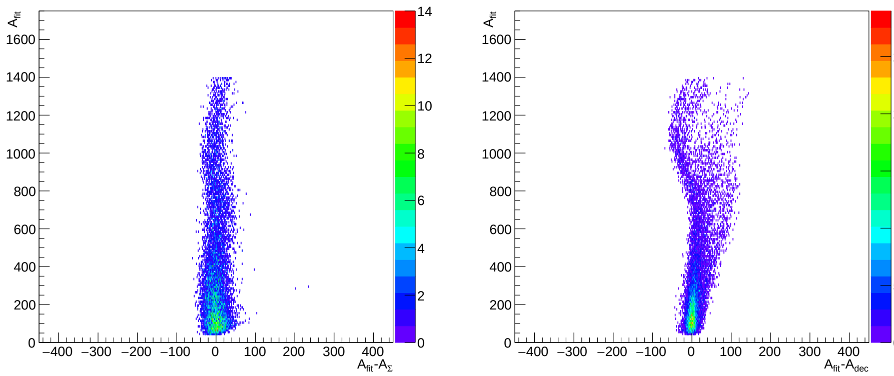

(a) (b)

Figure 6: Correlation between $A_{fit} - A_{\Sigma}$ and A_{fit} (a). Correlation between $A_{fit} - A_{dec}$ and A_{fit} (b).

In the study of these histograms, it can be seen that the developed alternative digital filtering scheme has practically no systematic deviations. Moreover, this scheme works better for amplitudes above the average. The signal deconvolution method has rather strong systematic deviations for amplitudes above the average but shows a very good result for small values of the signal amplitude. These conclusions were made from the study of the width of the spread of points along the $A_{fit} - A_{alternative}$ axis.

The above considerations were confirmed after the construction of the resolutions of methods relative to the base one (figure 7). Where $\sigma_{\epsilon} = RMS(\frac{A_{alternative} - A_{fit}}{A_{fit}})$. The resolution for small amplitudes or sums at the beginning of a histogram is better for the deconvolution method, but then the method of signal integration is better.

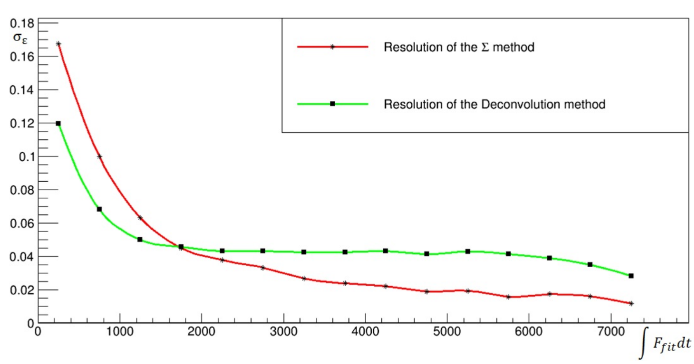

Figure 7: Relative fluctuations between digital filtering schemes.

4 Summary

The test beam data of the electromagnetic calorimeter prototype LumiCal were processed by the basic(Sect. 3.1) and two alternative methods(Sect. 3.2 and 3.3) of digital signal filtering. The developed signal integration scheme proved to be quite effective. It correlates well with the fittings, processes the data 150 times faster and can be included in the electronics of the detector as a firmware. Also this scheme does not have systematic deviations. The signal deconvolution method works well for small amplitude values, but it has systematic deviations at higher amplitudes.

Acknowledgements

The author are grateful to the supervision of A.Sapronov (JINR, Russia) and O.Borysov (Tel Aviv University, Israel) for execution of this work.

References

[1] Abramowicz, H. et al., *Forward Instrumentation for ILC Detectors* (arXiv:1009.2433 [physics.ins-det] DESY-10-142) 30 pages.

[2] Boland, M J et al.(CLIC and CLICdp Collaborations), *Updated baseline for a staged Compact Linear Collider* (arXiv:1608.07537 [physics.acc-ph] CERN-2016-004) 57 pages.

[3] FCAL Collaboration. LumiCal: http://fcal.desy.de/e107470/e107490/ .

[4] Szymon Kulis, *Development of prototype luminosity detector modules for future experiments on linear colliders* (Doctoral dissertation, Cracow, 2012) 175 pages.